Mineralogical Magazine, December 2010, Vol. 74(6), pp. 991–998

The crystal structure of munakataite, $Pb_2Cu_2(Se^{4+}O_3)(SO_4)(OH)_4$, from Otto Mountain, San Bernardino County, California, USA

A. R. KAMPF[1,*], S. J. MILLS[2] AND R. M. HOUSLEY[3]

[1] Mineral Sciences Department, Natural History Museum of Los Angeles County, 900 Exposition Boulevard, Los Angeles, CA 90007, USA

[2] Department of Earth and Ocean Sciences, University of British Columbia, Vancouver, British Columbia, Canada V6T 1Z4

[3] Division of Geological and Planetary Sciences, California Institute of Technology, Pasadena, CA 91125, USA

[*Received 13 November 2010; Accepted 2 December 2010*]

ABSTRACT

Munakataite, $Pb_2Cu_2(Se^{4+}O_3)(SO_4)(OH)_4$, has been found in association with a variety of rare secondary Te minerals at Otto Mountain, San Bernardino County, California, USA. It is very rare and occurs as subparallel bundles of blue needles up to 1 mm long. Electron microprobe analyses provided the empirical formula $Pb_{1.96}Cu_{1.60}[(Se^{4+}_{0.89}S_{0.11})_{\Sigma 1}O_3](SO_4)[(OH)_{3.34}(H_2O)_{0.66}]_{\Sigma 4}$. Munakataite is monoclinic, space group $P2_1/m$, with cell parameters a = 9.8023(26), b = 5.6751(14), c = 9.2811(25) Å, β = 102.443(6), V = 504.2(2) Å^3 and Z = 2. The crystal structure, solved by direct methods and refined to R_1 = 0.0308 for 544 $F_o > 4\sigma F$ reflections, consists of Jahn-Teller-distorted $Cu^{2+}O_6$ square bipyramids, which form chains along **b** by sharing *trans* edges across their square planes. The chains are decorated by SO_4 tetrahedra and $Se^{4+}O_3$ pyramids, which bond to apical corners of adjacent bipyramids. The chains are linked to one another *via* bonds to two different PbO_9 polyhedra, only one of which exhibits one-sided coordination typical of Pb^{2+} with a stereochemically active $6s^2$ lone-electron-pair. Munakataite is isostructural with schmiederite and the structure is closely related to that of linarite.

KEYWORDS: munakataite, schmiederite, selenite, sulphate, crystal structure.

Introduction

MUNAKATAITE is a very rare lead-copper selenite-sulphate first described by Matsubara *et al*. (2008) from a specimen collected on the dump of the Kato mine, Munakata City, Fukuoka Prefecture, Japan. It was found as aggregates of blue fibres up to only 30 μm in length. The chemical composition coupled with the similarity of the powder X-ray diffraction pattern to those of linarite, $PbCu(SO_4)(OH)_2$, and schmiederite, $Pb_2Cu_2(Se^{4+}O_3)(Se^{6+}O_4)(OH)_4$, and the similarity of the cell parameters to those of schmiederite led Matsubara *et al*. to conclude that munakataite is isostructural with schmiederite and has the ideal formula $Pb_2Cu_2(Se^{4+}O_3)(SO_4)(OH)_4$. The discovery of larger crystals of munakataite at Otto Mountain afforded the opportunity to collect structure data and determine the structure.

Occurrence

The munakataite crystal used in this study came from a specimen collected by one of the authors (RMH) at the Bird Nest drift on the southwest flank of Otto Mountain, ~2 km northwest of Baker, San Bernardino County, California. The Bird Nest drift (35º16.606′N, 116º05.956′W) is located 0.7

* E-mail: akampf@nhm.org
DOI: 10.1180/minmag.2010.074.6.991

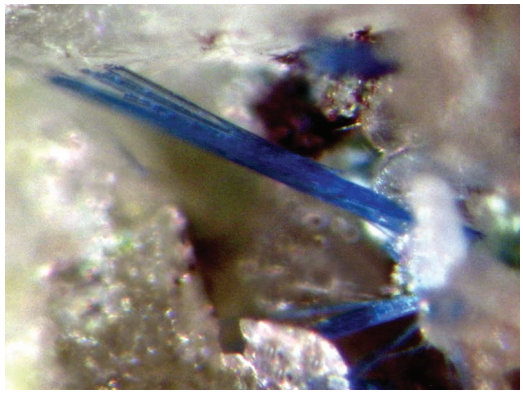

FIG. 1. Munakataite crystals on quartz; field of view – 2 mm. Joe Marty specimen and photo.

km northwest of the Aga mine (35º16.399′N, 116º05.665′W). Munakataite occurs as thin blue prismatic crystals (Fig. 1) up to 2 mm long on fracture surfaces and in small vugs in quartz veins in direct association with telluroperite (Kampf *et al*., 2010*f*) and caledonite. Other species identified in the Otto Mountain assemblages include acanthite, anglesite, atacamite, boleite, brochantite, burckhardtite, calcite, celestine, cerussite, chalcopyrite, bromine-rich chlorargyrite, chrysocolla, devilline, diaboleite, fluorite, fornacite, galena, gold, goethite, hessite, housleyite (Kampf *et al*., 2010*c*), iodargyrite, jarosite, khinite, kuranakhite, linarite, malachite, markcooperite (Kampf *et al*., 2010*d*), mimetite, mottramite, murdochite, muscovite, ottoite (Kampf *et al*., 2010*b*), paratimroseite (Kampf *et al*., 2010*e*), perite, phosphohedyphane, plumbojarosite, pyrite, schieffelinite, thorneite (Kampf *et al*., 2010*a*), timroseite (Kampf *et al*., 2010*e*), vanadinite, vauquelinite and wulfenite.

The unusual secondary Te minerals of the quartz veins are interpreted as having formed from the partial oxidation of primary sulphides (e.g. galena and chalcopyrite) and tellurides (e.g. hessite) during or following brecciation of the quartz veins. Munakataite is the only Se mineral identified thus far. The source of the Se is likely to be sulphides, in which it may be present in trace amounts, but the possible occurrence of a primary Se phase, such as clausthalite, cannot be discounted.

Chemical composition

Three analyses were conducted on munakataite at the California Institute of Technology using a JEOL 8200 electron microprobe operating in WDS mode. Analytical conditions were 20 kV, 5 nA and a focused beam. The standards were galena (Pb), Cu metal (Cu), Se metal (Se) and anhydrite (S). There was insufficient material for direct H_2O determination, so the H_2O content was calculated for charge balance in order to provide 11 O a.p.f.u. with S + Se = 2. Some beam damage was noted and this may account for the low CuO value. Semi-quantitative EDS analyses were consistent with near-stoichiometric amounts of Pb and Cu (Table 1).

The empirical formula for munakataite from Otto Mountain based upon 11 O and 2 S + Se a.p.f.u. is $Pb_{1.96}Cu_{1.60}[(Se^{4+}_{0.89}S_{0.11})_{\Sigma 1}O_3](SO_4)[(OH)_{3.34}(H_2O)_{0.66}]_{\Sigma 4}$. The empirical formula for munakataite from the Kato mine on the same basis is: $Pb_{2.00}(Cu_{1.92}Ca_{0.01})_{\Sigma 1.93}[(Se^{4+}_{0.99}S_{0.01})_{\Sigma 1}O_3](SO_4)[(OH)_{3.87}(H_2O)_{0.13}]_{\Sigma 4}$.

TABLE 1. Electron microprobe analyses (wt.%) of munakataite from the Kato mine (seven analyses) and Otto Mountain (five analyses).

	Kato mine (Matsubara *et al*., 2008)	Otto Mountain (this study)
PbO	53.71 (53.24–54.09)	55.00 (54.05–55.60)
CuO	18.33 (17.74–19.81)	16.05 (15.81–16.36)
CaO	0.04 (0.00–0.26)	none observed
SO3	9.73 (8.13–11.16)	11.22 (10.95–11.68)
SeO_2	13.19 (11.10–14.48)	12.42 (12.05–12.92)
H_2O*	4.47	5.25
Total	99.47	99.94

* Calculated to provide charge balance with 11 O and 2 S + Se a.p.f.u.

X-ray crystallography and structure refinement

Single-crystal X-ray data were obtained on a Rigaku R-Axis Rapid II curved image-plate microdiffractometer using monochromatized Mo-*K*α radiation. The Rigaku *CrystalClear* software package was used for processing the structure data, including the application of an empirical absorption correction using *ABSCOR* (Higashi, 2001). A numerical (shape-based) absorption correction using *NUMABS* (Higashi, 2000) was also attempted, but with inferior results. All non-hydrogen atoms were located by direct methods using *SIR92* (Altomare *et al.*, 1994). *SHELXL-97* software (Sheldrick, 2008) was used, with neutral atom scattering factors, for the refinement of the structure.

The munakataite crystals exhibited a high degree of mosaicity in the **c** direction, as shown by significant elongation and streaking of reflections. To minimize the effect of the mosaicity, a very small crystal (110 μm × 12 μm × 5 μm) was used for the data collection; this crystal still exhibited significant elongation of many reflections, however. Because of the small crystal size, reflection intensities fell off quickly above 20ºθ, severely limiting the dataset. Difficulties integrating the elongate reflections resulted in a relatively high R_{int} and are probably

TABLE 2. Crystallographic data and structure-refinement details for munakataite.

Crystal data	
Structural formula	$Pb_{1.93}Cu_{1.89}(Se^{4+}_{0.85}S_{0.15}O_3)(SO_4)(OH)_4$
Crystal system	Monoclinic
Space group	$P2_1/m$
Unit cell parameters *a*, *b*, *c* (Å), β (º)	9.802 (3), 5.675(1), 9.281(3), 102.443(6)
Volume (Å^3)	504.2(2)
Z	2
Density for above formula (g/cm^3)	5.305
Absorption coefficient (mm^{-1})	39.514
Crystal size (μm)	110 × 12 × 5
Data collection	
Diffractometer	Rigaku R-Axis Rapid II
Radiation, wavelength (Å)	Mo-*K*α, 0.71075
Temperature (K)	298
F(000)	706
θ range (º)	3.41 to 20.79
h, *k*, *l* ranges	±9, ±5, ±9
Axis, # frames, width (º), time (min.)	ω, 154, 5, 20
Reflections collected, unique	8377, 590 [R_{int} = 0.0807]
Unique reflections with $F_o > 4\sigma F$	544
Data completeness to θ_{max} (%)	98.8
Max. and min. transmission	0.8269 and 0.0978
Structure refinement	
Refinement method	Full-matrix least-squares on F^2
Data/restraints/refined parameters	590/4/106
Weighting coefficients *a*, *b* *	0, 22.0107
Final *R* indices [$F_o > 4\sigma F$]	R_1 = 0.0308, wR_2 = 0.0630
R indices (all data)	R_1 = 0.0340, wR_2 = 0.0647
Goodness-of-fit (GoF) on F^2	1.093
Largest diff. peak/hole (*e*/A^3)	+3.038 / −1.483

$R_{int} = \Sigma|F_o^2 - F_o^2(\text{mean})|/\Sigma[F_o^2]$. GoF = $S = \{\Sigma[w(F_o^2-F_c^2)^2]/(n-p)\}^{1/2}$ where n = no. of reflections, p = no. of refined parameters. $R_1 = \Sigma||F_o| - |F_c||/\Sigma|F_o|$. $wR_2 = \{\Sigma[w(F_o^2-F_c^2)^2]/\Sigma[w(F_o^2)^2]\}^{1/2}$. $w^* = 1/[\sigma^2(F_o^2) + (aP)^2 + bP]$ where P is $[2F_c^2 + \text{Max}(F_o^2,0)]/3$.

TABLE 3. Atomic coordinates and displacement parameters (Å^2) for munakataite.

	x	y	z	U_{eq}	U_{11}	U_{22}	U_{33}	U_{23}	U_{13}	U_{12}
Pb1	0.31694(9)	¼	0.41854(10)	0.0219(4)	0.0208(7)	0.0198(6)	0.0232(7)	0	0.0008(4)	0
Pb2	0.33579(10)	¼	0.97549(12)	0.0329(5)	0.0195(7)	0.0331(8)	0.0436(8)	0	0.0010(5)	0
Cu	0.9886(2)	−0.0002(3)	0.24421(19)	0.0148(9)	0.0221(14)	0.0079(13)	0.0137(12)	0.0001(9)	0.0024(9)	−0.0011(9)
Se	0.3597(2)	¾	0.2215(3)	0.0174(12)	0.0190(18)	0.0146(17)	0.0191(17)	0	0.0054(11)	0
S	0.3349(6)	¾	0.6883(6)	0.0172(18)	0.016(4)	0.010(3)	0.026(4)	0	0.006(3)	0
O11	0.376(2)	¾	0.0476(18)	0.045(5)	0.064(13)	0.049(13)	0.026(10)	0	0.020(9)	0
O12	0.2514(10)	0.5148(18)	0.2152(11)	0.023(3)	0.019(6)	0.021(7)	0.027(6)	0.003(5)	0.003(5)	−0.002(5)
O21	0.4828(15)	¾	0.7514(16)	0.028(4)	0.019(10)	0.039(11)	0.027(9)	0	0.009(7)	0
O22	0.3154(17)	¾	0.5248(15)	0.035(5)	0.041(11)	0.062(13)	0.000(8)	0	0.001(7)	0
O23	0.2690(11)	0.963(2)	0.7326(11)	0.031(3)	0.036(7)	0.026(7)	0.031(7)	0.006(6)	0.006(6)	0.008(6)
OH1	0.0260(15)	¾	0.3883(16)	0.018(4)	0.017(8)	0.014(9)	0.019(8)	0	−0.004(7)	0
H1	0.119(5)	¾	0.40(3)	0.050						
OH2	0.0775(15)	¼	0.3780(14)	0.016(4)	0.023(9)	0.016(9)	0.008(8)	0	0.000(7)	0
H2	0.06(3)	¼	0.470(11)	0.050						
OH3	0.0529(14)	¾	0.8975(16)	0.019(4)	0.007(8)	0.021(9)	0.023(9)	0	−0.009(7)	0
H3	0.141(10)	¾	0.95(2)	0.050						
OH4	0.0881(15)	¼	0.8924(14)	0.019(4)	0.029(9)	0.024(9)	0.002(8)	0	−0.004(7)	0
H4	0.07(3)	¼	0.984(12)	0.050						

Refined occupancies: Pb1: 0.976(14); Pb2: 0.958(14); Cu: 0.947(14); Se: 0.85(3):0.15(3) Se:S

responsible for the anomalous shapes of the displacement ellipsoids for several of the O atoms.

All non-hydrogen atoms were refined anisotropically at full occupancy in accord with the ideal formula, and the agreement index R_1 converged to 3.26%. Because the chemical analyses suggest that a small amount of S substitutes at the Se site and that Cu and Pb sites are not fully occupied, a refinement was attempted with both Se and S refined at the Se site and the occupancies of the Cu and Pb sites refined. This approach reduced R_1 to 3.10%. At this stage, examination of the difference-Fourier map indicated the likely site for all H atoms associated with the OH sites. The positions of the H atoms were constrained to a hydroxyl bond distance of 0.90(3) Å and their isotropic displacement parameters were held constant at 0.05 Å^2 in the final refinement, which converged to 3.08% for 544 $F_o > 4\sigma F$ reflections.

The details of the data collection and structure refinement are provided in Table 2. The final atomic coordinates, displacement parameters and occupancies are listed in Table 3. Selected interatomic distances are given in Table 4. A bond-valence analysis is provided in Table 5. Lists of observed and calculated structure factors have been deposited with the journal and can be downloaded from http://www.minersoc.org/pages/e_journals/dep_mat_mm.html.

Description of the structure

The munakataite structure (Fig. 2) consists of Jahn-Teller-distorted $Cu^{2+}O_6$ square bipyramids, forming chains along **b** by sharing *trans* edges across their square planes. The chains are decorated by SO_4 tetrahedra and $Se^{4+}O_3$ pyramids, which bond to apical corners of adjacent bipyramids. The chains are linked to one another *via* bonds to two different PbO_9 polyhedra. Munakataite is isostructural with schmiederite (Effenberger, 1987), in which the tetrahedron is centred by Se^{6+} and the structure is closely related to that of linarite (Schofield *et al.*, 2009), which has only SO_4 tetrahedra, instead of both SO_4 tetrahedra and SeO_3 pyramids. The structure type

TABLE 4. Selected bond distances (Å) and angles (º) for munakataite.

Pb1–OH2	2.296(14)	Pb2–OH4	2.384(15)
Pb1–O12 (×2)	2.389(10)	Pb2–O23 (×2)	2.743(11)
Pb1–O21	2.771(15)	Pb2–O21	2.764(15)
Pb1–O22 (×2)	3.005(5)	Pb2–O11	2.875(19)
Pb1–O23 (×2)	3.458(11)	Pb2–O11 (×2)	2.923(4)
Pb1–O22	3.528(16)	Pb2–O12 (×2)	2.947(10)
<Pb–O>	2.922	<Pb–O>	2.806
Cu–OH3	1.919(10)	Se–O11	1.656(16)
Cu–OH1	1.929(10)	Se–O12 (×2)	1.699(10)
Cu–OH4	1.942(9)	<Se–O>	1.685
Cu–OH2	1.962(9)		
Cu–O23	2.589(11)	S–O21	1.442(16)
Cu–O12	2.648(10)	S–O23 (×2)	1.471(12)
<Cu–O_{eq}>	1.938	S–O22	1.488(15)
<Cu–O_{ap}>	2.619	<S–O>	1.468

Hydrogen bonds (D = donor, A = acceptor)

D–H	*d*(D–H)	*d*(H···A)	<DHA	*d*(D···A)	A
OH1–H1	0.90(3)	2.04(14)	150(23)	2.85(2)	O22
OH2–H2	0.90(3)	1.72(9)	161(24)	2.58(2)	OH1
OH3–H3	0.90(3)	2.29(6)	170(23)	3.18(2)	O11
OH4–H4	0.90(3)	1.80(13)	150(23)	2.62(2)	OH3

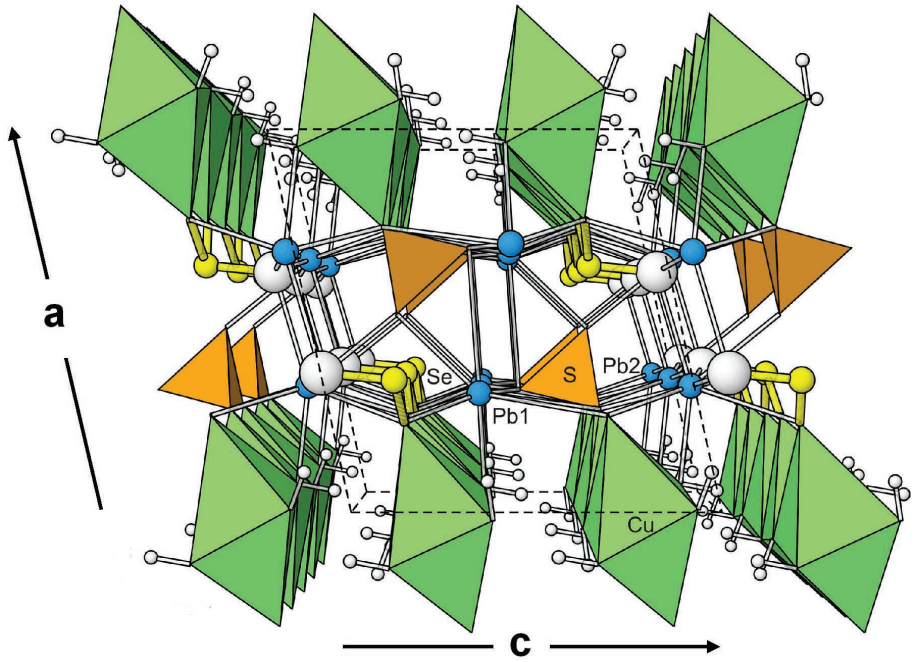

FIG. 2. Crystal structure of munakataite viewed in perspective along **b**.

has been described in detail by Effenberger (1987) and Schofield *et al*. (2009).

Both schmiederite and munakataite have **c** doubled compared to linarite, due to the ordered substitution of SeO_3 within the structure. The *a*, *b* and *c* cell parameters of munakataite are all slightly smaller than those observed in schmiederite, probably attributable to the difference in size between the SO_4 and SeO_4 tetrahedra. In the linarite structure, there is only one Pb site and it exhibits one-sided coordination typical of Pb^{2+} with a stereochemically active $6s^2$ lone-electron-

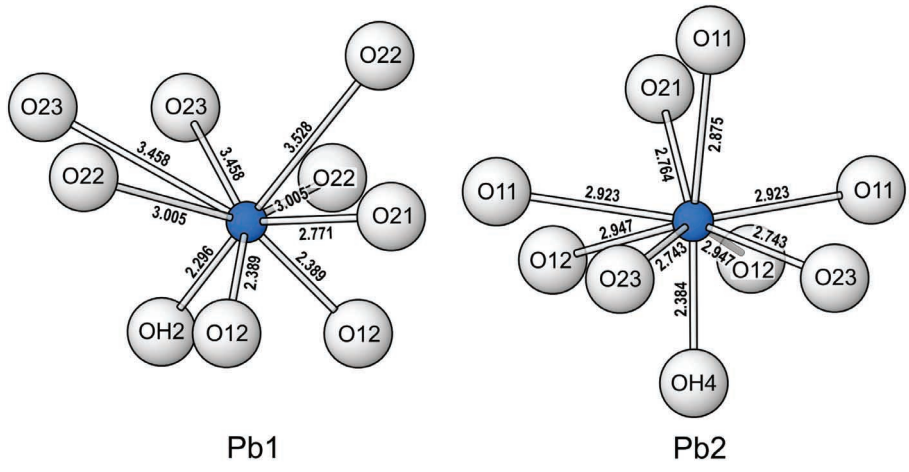

FIG. 3. Pb coordinations in munakataite.

TABLE 5. Bond-valence analysis for munakataite. Values are expressed in valence units.

	Pb1	Pb2	Cu	Se	S	H1	H2	H3	H4	Sum
O11		0.14 ×2→↓, 0.16		1.52				0.08		2.04
O12	0.42 ×2↓	0.13 ×2↓	0.07	1.35 ×2↓						1.97
O21	0.19	0.19			1.63					2.01
O22	0.12 ×2→↓, 0.04				1.44	0.11				1.83
O23	0.05 ×2↓	0.20 ×2↓	0.09		1.51 ×2↓					1.85
OH1			0.51 ×2→			0.89	0.22			2.13
OH2	0.51		0.47 ×2→				0.78			2.23
OH3			0.52 ×2→					0.92	0.19	2.15
OH4		0.42	0.49 ×2→						0.81	2.21
Sum	1.92	1.71	2.15	4.22	6.09	1.00	1.00	1.00	1.00	

Bond valences are based upon the ideal formula. Multiplicity is indicated by × →↓; Pb^{2+}—O bond strengths from Krivovichev and Brown (2001); Se^{4+}—O bond strengths from Brese and O'Keeffe (1991); Cu^{2+}—O and S^{6+}—O bond strengths from Brown and Altermatt (1985); hydrogen-bond strengths based on H···O bond lengths, also from Brown and Altermatt (1985).

pair. By contrast, the structures of munakataite and schmiederite each have two non-equivalent Pb sites (Fig. 3), only one of which, Pb1, exhibits one-sided coordination.

The H-atom positions in munakataite match closely with those determined by Schofield *et al*. (2009) for linarite. Furthermore, the hydrogen bonds based upon those H atom positions are consistent with those hypothesized by Effenberger (1987) for schmiederite.

Acknowledgements

Principal Editor Mark D. Welch and Associate Editor Fernando Cámara are thanked for their constructive comments on the manuscript. Joe Marty of Salt Lake City, Utah, USA is thanked for providing the image of munakataite. The EMP analyses were supported by a grant to the California Institute of Technology from the Northern California Mineralogical Association. The remainder of this study was funded by the John Jago Trelawney Endowment to the Mineral Sciences Department of the Natural History Museum of Los Angeles County.

References

Altomare, A., Cascarano, G., Giacovazzo, C., Guagliardi, A., Burla, M.C., Polidori, G. and Camalli, M. (1994) SIR92 – a program for automatic solution of crystal structures by direct methods. *Journal of Applied Crystallography*, **27**, 435.

Brese, N.E. and O'Keeffe, M. (1991) Bond-valence parameters for solids. *Acta Crystallographica*, **B47**, 192–197.

Brown, I.D. and Altermatt, D. (1985) Bond-valence parameters obtained from a systematic analysis of the inorganic crystal structure database. *Acta Crystallographica*, **B41**, 244–247.

Effenberger, H. (1987) Crystal structure and chemical formula of schmiederite $Pb_2Cu_2(OH)_4(SeO_3)(SeO_4)$, with a comparison to linarite $PbCu(OH)_2(SO_4)$. *Mineralogy and Petrology*, **36**, 3–12.

Higashi, T. (2000) *NUMABS*. Rigaku Corporation, Tokyo, Japan.

Higashi, T. (2001) *ABSCOR*. Rigaku Corporation, Tokyo, Japan.

Kampf, A.R., Housley, R.M. and Marty, J. (2010*a*) Lead-tellurium oxysalts from Otto Mountain near Baker, California: III. Thorneite, $Pb_6(Te_2^{6+}O_{10})(CO_3)Cl_2(H_2O)$, the first mineral with edge-sharing tellurate dimers. *American Mineralogist*, **95**, 1548–1553.

Kampf, A.R., Housley, R.M., Mills, S.J., Marty, J. and Thorne, B. (2010*b*) Lead-tellurium oxysalts from Otto Mountain near Baker, California: I. Ottoite, Pb_2TeO_5, a new mineral with chains of tellurate octahedra. *American Mineralogist*, **95**, 1329–1336.

Kampf, A.R., Marty, J. and Thorne, B. (2010*c*) Lead-tellurium oxysalts from Otto Mountain near Baker, California: II. Housleyite, $Pb_6CuTe_4O_{18}(OH)_2$, a new mineral with Cu-Te octahedral sheets. *American Mineralogist*, **95**, 1337–1342.

Kampf, A.R., Mills, S.J., Housley, R.M., Marty, J. and Thorne, B. (2010*d*) Lead-tellurium oxysalts from Otto Mountain near Baker, California: IV. Markcooperite, $Pb_2(UO_2)Te^{6+}O_6$, the first natural uranyl tellurate. *American Mineralogist*, **95**, 1554–1559.

Kampf, A.R., Mills, S.J., Housley, R.M., Marty, J. and Thorne, B. (2010*e*) Lead-tellurium oxysalts from Otto Mountain near Baker, California: V. Timroseite, $Pb_2Cu_5^{2+}(Te^{6+}O_6)_2(OH)_2$, and paratimroseite, $Pb_2Cu_4^{2+}(Te^{6+}O_6)_2(H_2O)_2$, new minerals with edge-sharing Cu-Te octahedral chains. *American Mineralogist*, **95**, 1560–1568.

Kampf, A.R., Mills, S.J., Housley, R.M., Marty, J. and Thorne, B. (2010*f*) Lead-tellurium oxysalts from Otto Mountain near Baker, California: VI. Telluroperite, $Pb_3Te^{4+}O_4Cl_2$, the Te analogue of perite and nadorite. *American Mineralogist*, **95**, 1569–1573.

Krivovichev, S.V. and Brown, I.D. (2001) Are the compressive effects of encapsulation an artifact of the bond valence parameters? *Zeitschrift für Kristallographie*, **216**, 245–247.

Matsubara, S., Mouri, T., Miyawaki, R., Yokoyama, K. and Nakahara, M. (2008) Munakataite, a new mineral from the Kato mine, Fukuoka, Japan. *Journal of Mineralogical and Petrological Sciences*, **103**, 327–332.

Schofield, P.F., Wilson, C.C., Knight, K.S. and Kirk, C.A. (2009) Proton location and hydrogen bonding in the hydrous lead copper sulfates linarite, $PbCu(SO_4)(OH)_2$, and caledonite, $Pb_5Cu_2(SO_4)_3CO_3(OH)_6$. *The Canadian Mineralogist*, **47**, 649–662.

Sheldrick, G.M. (2008) A short history of SHELX. *Acta Crystallographica*, **A64**, 112–122.